

FAST ANALYSIS OF MMF HARMONICS CONTENT IN THREE-PHASE ELECTRICAL MACHINES

Gheorghe MADESCU¹, Erhard BERWANGER², Marius BIRIESCU³, Martian MOT³

¹ Romanian Academy – Timisoara Branch, Romania

² Ludwigsburg, Germany

³ Politehnica University of Timisoara, Romania

Corresponding author: Martian MOT, E-mail: martian.mot@upt.ro

Abstract. Fractional-slot windings, tooth-concentrated windings, multilayer windings and other “new” windings have been gained a great interest over the last years due to some advantages that this type of windings provides for synchronous permanent magnet machines. In spite of their advantages, these windings exhibit high content of space harmonics in the air-gap magneto-motive force (MMF) distribution that can give rise unwanted effects in a.c. electrical machines. This paper aims to help the machine designer to select the proper winding configurations and to sort out the best winding layout. Firstly, the paper reminds the theoretical concepts based on star of slots and Fourier-series expansion of the air-gap MMF wave used to compute the winding characteristics. This classical method was implemented on the computer to quickly determine the values of the main winding factor, space harmonic content and differential leakage coefficient in order to identify the optimal winding structure. Thus, the proposed application becomes a helpful tool in the design process and can be applied for any type of single or three-phase winding layout irrespective of number of layer or number of conductor per slot. The paper also describes how to use this new and original application that is free available on the website (<http://acad-tim.tm.edu.ro/FastMMF/>).

Key words: fractional-slot windings, magnetomotive force (MMF) optimization, multilayer windings, space harmonic amplitudes, winding factor, windings in a.c. machines

1. INTRODUCTION

The electrical machines designer knows very well that the winding arrangement strongly and directly affects the machine performance. So, in the predesign stage, it is very important to choose a suitable winding structure with optimal characteristics. There are different machine designs with various winding structures and different pole/slot number combinations. Even if the pole/slot ratio is fixed, there is the possibility to choose the number of layer and the coil pitch. An unsuitable winding configuration can give rise to unwanted effects in AC electrical machines like [1]: oversaturation of the core and additional core losses, higher inductances, overheating, parasitic torques, unbalanced radial magnetic forces, noise and vibrations, etc.

Generally, an improper winding choice produces a higher magneto-motive force (MMF) harmonic content that may be so high to cause also a degrading of the machine power. It is well known that distributed overlapping windings used for classical synchronous or asynchronous machines results in a more sinusoidal air-gap MMF distribution. However, the slot-concentrated windings for low-speed permanent magnet machines have been gaining a great interest over the last years [2, 3, 4, 5, 6]. That is why the windings performances analyses or winding layouts optimization are becomes again a very important and timely subject in this field [6, 7, 8, 9]. The paper [6] analyzes the impact of different space harmonics caused by air-gap MMF distribution on the rotor losses and highlights that the sub-harmonics have a dominant effect and are the main causes of rotor losses.

Also, in order to reduce the space harmonic content and improve the winding performance, the papers [10, 11, 12, 13] propose to use different number of conductors per machine slots (unequal-turn coils); the authors in [13] propose a design program flowchart to optimize the turn number of the coils.

Because the tooth concentrated windings generate some additional and specifically problems, some authors try to introduce “new concepts” and “new methods” to analyze these “new” windings. In the paper [14] are made some appreciations about the “new” terminology in this field “in order to prevent the wander of the defined notions from the classical acceptance”. Cistelean *et al.* [14] state that “these windings do not need any new methods and no new methods can be claimed. The classical star of the slots is perfectly valid even for these “new” concentrated windings”.

From the classical theory it is known that the winding performances are represented by some characteristics: the main winding factor, the harmonic content (amplitudes of each MMF space harmonic) and differential leakage coefficient. These characteristics [15] are generally used in the predesign stage in order to sort out the different winding layout and to find the best winding structure.

The paper reminds the classical method based on star of slots and Fourier-series expansion of the air-gap MMF wave used to compute the winding characteristics. The method has been implemented on computer for quickly find the values of the main winding factor, harmonic content and differential leakage coefficient for any type of single or three-phase windings layout irrespective of number of layers or number of conductors per slot. The main objective of this paper is to present the theoretical basis of this program and how to use this application that is free available on the website.

2. THE AIR-GAP MMF WAVE

A stator winding must be arranged to utilize as fully as possible the stator periphery in order to obtain the greatest air-gap flux density. For this purpose, it is favorable to distribute each side of the coils in several slots. But this distribution of the AC winding in the slot is “more an art than a science” [16]. If no unipolar fluxes pass through machine air-gap and $A(\theta)$ is the distribution of the current layer intensity along the outer side of the air-gap, than the distribution curve of the magnetomotive force is defined by the relation [17]:

$$F(\theta) = \delta \cdot H_{\theta} = \int_0^{\theta} A(\theta) d\theta \quad , \quad (1)$$

where: δ is the length of a constant air-gap and H_{θ} is the magnetic field intensity at the point having the coordinate θ . In this relation the iron core with infinite magnetic permeability is assumed.

Because the winding coils are placed inside the machine slots the magnetomotive force is a stepped curve with the steps situated exactly in the slot axes. That means that the effect of slotting is disregarded (the slot openings are neglected in order to highlight firstly the influence of the winding arrangement). In consequence, the both MMF and air-gap flux density curves are not sinusoidal waves. Due to the discrete position of the winding coils inside the slots, the air-gap MMF at the time t , according with (1) is:

$$F(k, t) = \sum_{\lambda=1}^k A(\lambda, t) \quad , \quad (2)$$

where: $A(\lambda, t)$ is the total current intensity (at the time t) within the λ -order slot and $F(k, t)$ is the air-gap MMF in the axis of k -order slot, at the time t . From this equation the MMF stepped curves can be described by a matrix that has a number of elements equals to the slot number of the stator.

Thus, for the computing of total air-gap MMF wave form it is necessary to know the current distribution in all the stator slots. At the symmetrical three-phase induction machine, the phase windings distributions are usually identical in layout being space-displaced by 120° electrical degree from each other. So, the layout of one phase is enough to draw MMF waveform.

In this purpose it is convenient to use the classical concept [17] of coils with “go-side” and “return-side” placed within the slots. A unidimensional matrix has to describe the winding distribution because one intends to implement the method on the computer. According to (2) the air-gap MMF at the instant of time can be computed if the current intensity distribution within the slots of one phase is known.

Firstly, on define this phase current matrix \mathbf{A} that consist of Z -number of elements equal to slot number of the machine. Each element of this matrix is equal to per unit filling degree of the corresponding slot and the sign (\pm) is assigned according to “go-side” or “return-side” of the coils. In Fig. 1 it is presented three cases of phase winding arrangement with all the phase coils series connected.

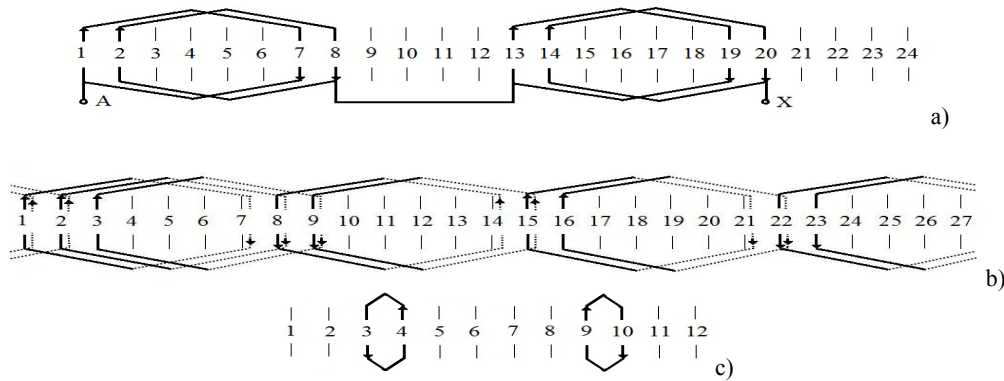


Fig. 1 – Different phase winding layout: a) Single layer winding (24slots/4poles configuration); b) Double layer winding (27slots/4poles configuration); c) Single layer tooth-concentrated winding (12slots/10poles).

Case 1 in Fig. 1a: Single winding layer; $Z = 24$ slots; $2p = 4$ poles; $q = 2$ slots per pole per phase. According to the phase winding layout from Fig. 1a the phase current matrix is: $\mathbf{A} = [1, 1, 0, 0, 0, 0, -1, -1, 0, 0, 0, 0, 1, 1, 0, 0, 0, 0, -1, -1, 0, 0, 0, 0]$, because all the four coils of the phase have the same number of turns. It is easy to see the correspondence between the elements of matrix \mathbf{A} and the phase layout from Fig. 1a. The matrix elements have zero-values if there are no current within the corresponding slots. For instance, $\mathbf{A}(2) = 1$, $\mathbf{A}(3) = 0$, $\mathbf{A}(7) = -1$, $\mathbf{A}(13) = 1$.

Case 2 in Fig. 1b: Double layer winding; 27 slots; 4 poles; $q = 2.25$ slots per pole per phase. For this case the corresponding matrix is: $\mathbf{A} = [2, 2, 1, 0, 0, 0, -1, -2, -2, 0, 0, 0, 0, 1, 2, 1, 0, 0, 0, 0, -1, -2, -1, 0, 0, 0, 0, 0]$. The first slot is completely filled by two sides of two different coils; so, the first matrix element has the value “2” that means 100% slot filled. The third slot includes only one coil side and thus the corresponding matrix element has the value “1” that means 50% slot filled. Instead of the value “2” and “1”, in the matrix \mathbf{A} one can use the values “4” and “2”, or others integer numbers.

Case 3 in Fig. 1c: Single layer – tooth concentrated winding; 12 slots; 10 poles; $q = 0.4$ slots per pole per phase. The phase consists of only two coils (tooth concentrated coils). The corresponding matrix \mathbf{A} can be written very easy: $\mathbf{A} = [0, 0, -1, 1, 0, 0, 0, 0, 1, -1, 0, 0]$.

Secondly, knowing the current distribution matrix of one phase, using (2) one can obtain the elements of $\mathbf{MF1}$ matrix corresponding to the phase “1”, at the time $t = 0$ for instance:

$$\begin{aligned} \mathbf{MF1}(1) &= \mathbf{A}(1); & \mathbf{MF1}(2) &= \mathbf{A}(1) + \mathbf{A}(2); \\ \mathbf{MF1}(3) &= \mathbf{A}(1) + \mathbf{A}(2) + \mathbf{A}(3); & \dots & \dots \dots \dots \mathbf{MF1}(Z) = \sum_{\lambda=1}^Z \mathbf{A}(\lambda), \end{aligned} \tag{3}$$

Owing to symmetry, the matrix $\mathbf{MF2}$ and the matrix $\mathbf{MF3}$ can be obtained very easy by changing the place of the elements of the matrix $\mathbf{MF1}$. For generality, the elements of the matrix $\mathbf{MF2}$ are displaced with $Z/3$ positions and for $\mathbf{MF3}$ the displacement is $2Z/3$, excepting the cases in which $p = 3k$, $k = 1, 2, 3, \dots$, when the displacement is $Z/3p$ and $2Z/3p$.

Finally, the resultant air-gap MMF is the sum of the three air-gap magnetomotive forces (at the instant of time t) corresponding to the each phase. But, the currents of the three-phase machine are time delayed by $2\pi/3$. Thus, the resultant \mathbf{MF} matrix can be calculated as follows:

$$\mathbf{MF} = \mathbf{MF1} \cdot \cos \omega t + \mathbf{MF2} \cdot \cos \left(\omega t - \frac{2\pi}{3} \right) + \mathbf{MF3} \cdot \cos \left(\omega t - \frac{4\pi}{3} \right). \tag{4}$$

Without loss of generality, the calculation below was made always at the time $t=0$, when the current i_1 in phase “1” is maxim and $i_2 = i_3 = -0.5 i_1$. In consequence, the last relation, in per-unit, becomes:

$$\mathbf{MF} = \mathbf{MF1} - \frac{1}{2}\mathbf{MF2} - \frac{1}{2}\mathbf{MF3}. \tag{5}$$

For instance, in the above Case 2 the current matrix \mathbf{A} with 27 elements is known. Using this matrix, with (3) one can obtains the $\mathbf{MF1}$ matrix corresponding to the phase “1” having the following elements (Fig. 2.a):

$\mathbf{MF1} = [2, 4, 5, 5, 5, 5, 4, 2, 0, 0, 0, 0, 0, 1, 3, 4, 4, 4, 4, 4, 3, 1, 0, 0, 0, 0, 0]$. In the next stage, both $\mathbf{MF2}$ and $\mathbf{MF3}$ matrices are obtained directly by displacement with $Z/3 = 9$, respectively $2Z/3=18$ positions of the elements of $\mathbf{MF1}$. Finally, with (5) results: $\mathbf{MF} = [0, 2, 3.5, 4.5, 4.5, 3.5, 2, 0, -2, -3, -4, -4, -3, -1.5, -0.5, 2, 3, 4, 3, 2, 0.5, -1.5, -3, -4, -4, -3, -2]$. The matrix of one phase $\mathbf{MF1}$ or the resultant \mathbf{MF} matrix allows to draw the air-gap MMF waveform that is a stepped curve. Figure 2 shows how to use the elements of the matrix $\mathbf{MF1}$ or \mathbf{MF} to draw these stepped functions.

The number of matrix element corresponds to the number of slots and to the number of function steps. In the Fig. 2a can be see the correspondence between few matrix elements and the curve steps. Of course, some “steps” of curve can have zero-value.

According to the above remarks, the air-gap MMF space distribution at the instant of time can be considered as a mathematical function and can be expressed as the following stepped function:

$$F(\theta) = \begin{cases} \mathbf{MF}(1), & 0 \leq \theta < \alpha \\ \mathbf{MF}(2), & \alpha \leq \theta < 2\alpha \\ \mathbf{MF}(3), & 2\alpha \leq \theta < 3\alpha \\ \dots\dots\dots \\ \mathbf{MF}(Z), & (Z-1)\alpha \leq \theta < 2\pi \end{cases} \quad (6)$$

where: $\alpha = 2\pi/Z$ is the angular displacement between two adjacent slots considering a regular distribution of the slots.

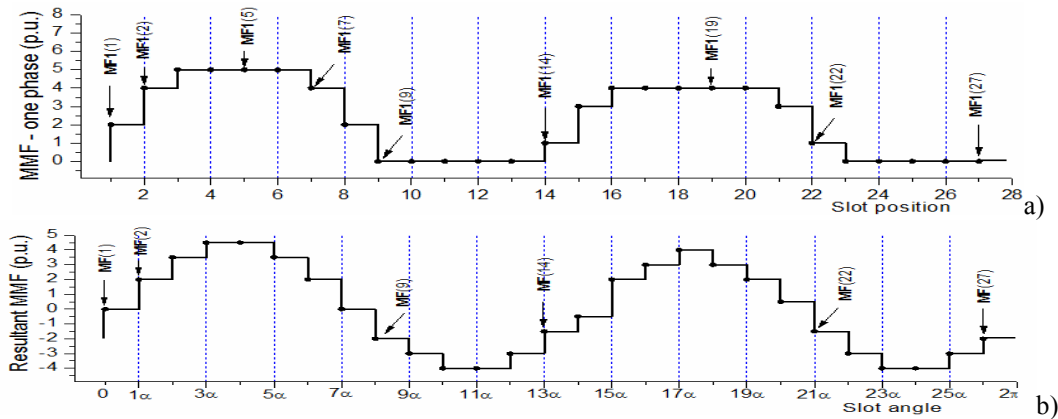


Fig. 2 – Airgap MMF waveforms as stepped functions: a) MMF corresponding to phase “1”; b) resultant MMF wave as sum of the three phases ($i_2 = i_3 = -0.5 i_1$).

3. THE AIR-GAP MMF HARMONICS CONTENT

The stepped curves in Fig. 2 highlight that the air-gap resultant MMF waveform is more sinusoidal than the MMF for one phase, but both waves differ from sinusoidal. For this reason in the AC machine air-gap there are a significant MMF space harmonics content.

The function described by (6) can be easy expanded as a Fourier series in order to assess the MMF space harmonics. In the general case of a periodical function $F(\theta)$, the very well-known harmonic relations of Fourier-series expansion are:

$$F(\theta) = \sum_{\mu=1}^{\infty} (A_{\mu} \cos \mu\theta + B_{\mu} \sin \mu\theta) = \sum_{\mu=1}^{\infty} M_{\mu} \sin(\mu\theta + \beta_{\mu}), \quad (7)$$

where M_{μ} and β_{μ} are the amplitude and the initial phase of the harmonic of μ -order:

$$M_{\mu} = \sqrt{A_{\mu}^2 + B_{\mu}^2}; \quad \beta_{\mu} = \arctan \frac{B_{\mu}}{A_{\mu}}, \quad (8)$$

with the assumption that there is no constant term in this series. In the particular case of step function (6) the amplitudes A_{μ} and B_{μ} from (7) can be expressed using the elements of resultant \mathbf{MF} matrix as follows:

$$A_\mu = \frac{1}{\mu\pi} \sum_{i=1}^Z \mathbf{MF}(i) [\sin(i\alpha\mu) - \sin((i-1)\alpha\mu)]; \quad B_\mu = -\frac{1}{\mu\pi} \sum_{i=1}^Z \mathbf{MF}(i) [\cos(i\alpha\mu) - \cos((i-1)\alpha\mu)]. \quad (9)$$

The sums (9) are made along the entire bore of the machine to which corresponds the air-gap periphery angle of 2π . From this reason μ is called the mechanical harmonic order.

In consequence, the first harmonic of the lowest order $\mu = 1$ forms a one pole-pair wave corresponding to the entire air-gap periphery. If the machine has p -pole pairs, the space harmonic producing a MMF wave with p -pole pairs is called the working harmonic [17], or the main harmonic and is of the order $\mu = p$. Related to this working harmonic, all the wave of order $\mu > p$ are called upper space harmonics and all the wave with $\mu < p$ are called subharmonics. So, the harmonic of order $\mu = 1$ has one pole-pair, the harmonic of order $\mu = 2$ has two pole-pair, and of the order $\mu = p$ has p pole-pair, and so on.

For particular case of integer slot windings (integer number of slots per pole per phase) there are no subharmonics and beside the working harmonic $\mu = p$ there exists upper harmonics only of order: $\mu = 5p$, $\mu = 7p$, $\mu = 11p$, $\mu = 13p, \dots$, $\mu = (6k+1)p$, $k = 0, \pm 1, \pm 2, \dots$. For instance, in order to clarify the space harmonic types that arise in the air-gap MMF wave, one consider the above three phase winding ($p = 2$) with phase distribution in Fig. 1b and resultant MMF distribution in Fig. 2b. At the instant $t = 0$ and using (8) and (9) the MMF harmonic amplitudes up to the harmonic of order $\mu = 214$ are presented in Table 1.

Because this winding is a fractional slot winding ($q = 2.25$) in the MMF harmonic spectrum (Table 1) there exist all types of the harmonics (the working harmonic of order $\mu/p = 1$, with the amplitude considered of 100%; the subharmonic of order $\mu/p = 1/2$, with amplitude $M_1 = 11.06\%$ related to working harmonic; even harmonics: $\mu/p = 4/2$, $\mu/p = 8/2$, etc.; fractional harmonics: $\mu/p = 5/2$, $\mu/p = 7/2$, etc.; the first "step harmonics": $\mu/p = 25/2$, $\mu/p = 29/2$ are the harmonics of order $\mu/p = (Z \cdot k \pm p)/p$ with $k = 1$; the second "step harmonics": $\mu/p = 52/2$, $\mu/p = 56/2$, with $k = 2$).

Table 1

Orders and Space Harmonic Amplitudes [%]; case of Fig. 1b

μ	1	2	4	5	7	8	10	11	13	14	16	17	20	25	29
$v=\mu/p$	1/2	1	2	5/2	7/2	4	5	11/2	13/2	7	8	17/2	10	25/2	29/2
M_μ [%]	11.1	100	1.02	1.35	1.99	0.98	2.65	1.18	0.78	0.73	0.81	1.56	0.7	8.0	6.9
μ	37	44	52	56	79	83	106	110	133	137	160	164	187	191	214
$v=\mu/p$	37/2	22	26	28	79/2	83/2	53	55	133/2	137/2	80	82	187/2	191/2	107
M_μ [%]	0.72	0.6	3.85	3.57	2.53	2.41	1.89	1.82	1.5	1.46	1.25	1.22	1.07	1.05	0.93

One can be seen in Table 1 that the highest upper harmonics are the step harmonics. The amplitudes of these harmonics are depending of the number of slots and not depending of the winding type. The step harmonic of order $\mu = 25$ has an amplitude $M_{25} = 8.0\%$ related to working harmonic.

The space harmonic content of the air-gap MMF can be characterized by the differential leakage reactance coefficient (σ_0). According with [16, 17] this coefficient can be calculated by means of harmonic amplitudes with the relation:

$$\sigma_0 = \frac{1}{M_p^2} \cdot \sum_{\mu=1}^{\infty} M_\mu^2 - 1, \quad (10)$$

where M_μ and M_p are the amplitude of μ -order harmonic and respectively of main harmonic $\mu = p$.

Because all the MMF harmonic amplitudes are known, is very easy to use (10) in order to assess σ_0 -coefficient. In the presented case (Fig. 1b), the value is $\sigma_0 = 0.032917$.

4. THE MAIN WINDING FACTOR

Beside the differential leakage reactance coefficient (σ_0), the main winding factor (k_w) is a significant criterion for the winding design. The electromagnetic torque of an electrical machine is proportional to this winding factor. In consequence, a low winding factor has to be compensated with more number of turns or higher current.

To calculate this winding factor corresponding to main MMF wave one use the classical star of slots method with the defined notions from the classical acceptance. It is very well known that this star of slots represents the phasors of electromotive force (EMF) induced in each coil side placed in the stator slots. Some details about use the star of slot in windings design and in harmonics determination are reported in [18]. Owing to the phase symmetry the main winding factor can be calculated using only one phase.

The electrical periodicity of the winding is represented by the greatest common divisor (GCD) between the number of slots and the number of pole pairs (p). For instance, in the Case 1 in Fig. 1a the greater common divisor between the number of slot ($Z = 24$) and the number of pole pairs ($p = 2$) is $GCD = 2$ and the star of slots has 12 spokes (Fig. 3).

According to Fig. 1a the spokes corresponding to phase A are: (1, 2, 7, 8, 13, 14, 19, 20). Assuming a same turns number in each slot, the corresponding EMF phasors are: $\underline{E}_1 = E e^{jp\alpha_1}$; $\underline{E}_2 = E e^{jp\alpha_2}$; $\underline{E}_7 = -E e^{jp\alpha_7}$; $\underline{E}_8 = -E e^{jp\alpha_8}$ and so on; the angle $p\alpha_i$ is the electrical angle of the i -EMF phasor, and α_i is the mechanical slot angle of the i -slot; the sign (\pm) depending on the current sense in the respective slot.

The winding factor is defined as the ratio between modulus of geometrical sum of the EMF phasors and the arithmetical sum of EMF phasors modulus. In consequence, the winding factor for this case will be:

$k_w = |\underline{E}_{sum}|/8E$, where:

$$\underline{E}_{sum} = E \left(e^{jp\alpha_1} + e^{jp\alpha_2} - e^{jp\alpha_7} - e^{jp\alpha_8} + e^{jp\alpha_{13}} + e^{jp\alpha_{14}} - e^{jp\alpha_{19}} - e^{jp\alpha_{20}} \right). \quad (11)$$

On the contrary, in Case 2 in Fig. 1b the greater common divisor between $Z = 27$ and $p = 2$ is $GCD = 1$, and in consequence there is no periodicity of the winding and the star of slots has 27 spokes (Fig. 4).

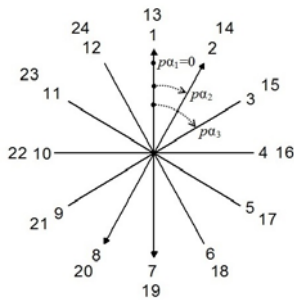


Fig. 3 – Star of slots for the case in Fig. 1a.

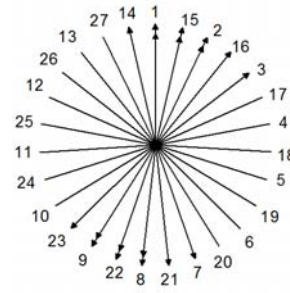


Fig. 4 – Star of slots for the case in Fig. 1b.

In this figure only the EMF phasors corresponding to one phase are marked. For the same reason as in the first case all the EMF phasors $E_7, E_{21}, E_8, E_{22}, E_9, E_{23}$ have the sign (-). Finally:

$$\underline{E}_{sum} = E \left(e^{jp\alpha_{14}} + 2e^{jp\alpha_1} + 2e^{jp\alpha_{15}} + 2e^{jp\alpha_2} + e^{jp\alpha_{16}} + e^{jp\alpha_3} - e^{jp\alpha_7} - e^{jp\alpha_{21}} - 2e^{jp\alpha_8} - 2e^{jp\alpha_{22}} - 2e^{jp\alpha_9} - e^{jp\alpha_{23}} \right), \quad (12)$$

and: $k_w = |\underline{E}_{sum}|/18E$.

Beside of the old technical literature, recent papers [7, 11, 18] uses the star of slots method in winding analysis. It is understood that the star of slot allows calculating the winding factor of the working harmonic if the phase winding diagram layout is given.

5. THE APPLICATION OF THE FastMMF

The program **FastMMF** allows the calculation of winding characteristics on the basis of the star of slots theory and Fourier-series expansion of the air-gap MMF wave according to above considerations in this paper. **FastMMF** is original free software (<http://acad-tim.tm.edu.ro/FastMMF/>) and is distributed in the hope that it will be useful in the electrical machines design process.

As an example, the program starts with input data (Fig. 5) which are the number of pole pairs, the number of slots, the number of phases (1 or 3), minimum amplitude of displayed harmonics and phase current matrix.

Fast MMF

Fast Analysis of MMF Harmonics Content in AC Electrical Machines

Description	Input Field
Number of Pole Pairs	<input type="text" value="5"/>
Number of Slots	<input type="text" value="12"/>
Number of Phases	<input type="text" value="3"/>
Minimum Amplitude of Displayed Harmonics, %	<input type="text" value="5"/>
Phase Current Matrix	<input type="text" value="0-12-10 0 0 1-2 1 0 0"/>

Fig. 5 – Input data for a specific winding.

Results

Filling of the slots: 2 2 2 2 2 2 2 2 2 2 2 2

Differential leakage reactance coefficient = 0.967301

Main winding factor = 0.933013

Amplitude(5) = 0.712769 p.u.

The order and the amplitude of each MMF Space Harmonic:

1 : 35.90
 -5 : 100.00
 7 : 71.43
 -17 : 29.41
 19 : 26.32
 -29 : 17.24
 31 : 16.13
 -41 : 12.20
 43 : 11.63
 -53 : 9.43
 55 : 9.09
 -65 : 7.69
 67 : 7.46
 -77 : 6.49
 79 : 6.33
 -89 : 5.62
 91 : 5.49

The resultant MF-matrix (air-gap MMF wave), p.u.:

0.50 -1.00 1.00 -0.50 0.50 0.50 -0.50 1.00 -1.00 0.50 -0.50 -0.50

Fig. 6 – The results for the preset input data.

In some specific cases if the Fig. 7 becomes not clearly (many harmonics overlapped) there is the possibility to exclude the harmonics that have small amplitudes; in this purpose we must repeat the calculation (reload the page) and increase the input data value “Minimum Amplitude of Displayed Harmonics”. As a result in Fig. 7 remain only the few significant harmonic orders with clear representation.

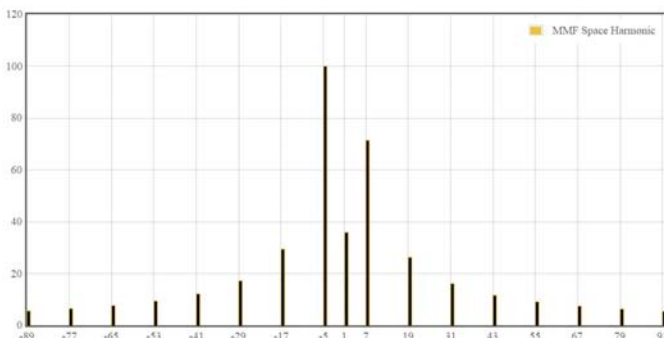


Fig. 7 – The orders and the amplitudes of the MMF space harmonics with the numerical results in Fig. 6.

The amplitudes of the MMF space harmonics up to order $\mu = 4000$ are computed, but most of them have very small amplitudes (some harmonic orders are still absent). To reduce the number of displayed harmonics a limit (minimum amplitude) for the displayed harmonics was imposed; in Fig. 5 this limit is set to 5%. Between the elements of phase current matrix has to be a blank space. Enter all the requested data for other specific case and press the “Calculate” button. To repeat the calculations reload the page. With the preset input data in Fig. 5 one obtains the results presented in Fig. 6.

These results refer to:

- filling of the slots (these numbers must be equal; if not, that means that there is a mistake in the phase winding layout, respectively in the current matrix, or the winding is not feasible as three-phase symmetrical winding);
- differential leakage reactance coefficient (σ_0);
- main winding factor (k_w);
- amplitude of the main harmonic (this case $\mu = 5$);
- the order and the amplitude of each MMF space harmonic (one can see displayed only the harmonics of amplitudes higher than 5% according to the input data);
- the resultant MF-matrix that represents the stepped function of air-gap MMF wave.

The results calculated in Fig. 6 are plotted respectively in Fig. 7 and Fig. 8.

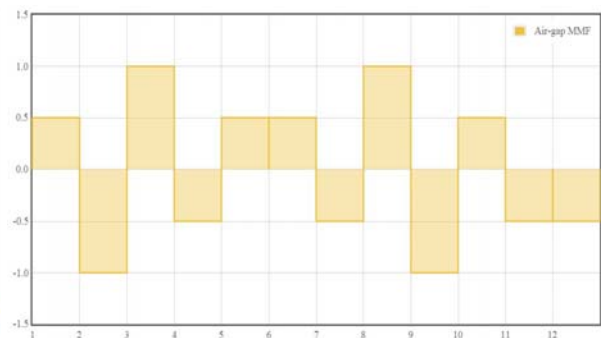


Fig. 8 – The air-gap MMF stepped wave with the numerical results in Fig. 6.

Now, the program provide the possibility to compute the cases with single-phase windings ($m = 1$) and three-phase windings ($m = 3$), but the next version of this program will be extended for some significant cases with $m > 3$.

6. CONCLUSIONS

This paper shortly reminds the classical method based on star of slots and Fourier-series expansion of the air-gap MMF wave in electrical machines and proves that this method is suitable to compute the winding characteristics of any type of a.c. winding irrespective of number of layer, number of conductors per slot, number of phases, number of slots/pole/phase. However, this classical method is rather complicated for computer implementation that is the main drawback of the method.

From this reason the authors propose a new software based on this method for quickly find the values of the main winding factor, amplitudes of each MMF space harmonics (including subharmonics), differential leakage coefficient, air-gap MMF wave, and for checking the feasibility of the winding layout.

This application is free available on the website and will provide researchers and engineers a helpful tool to quickly compute the a.c. winding characteristics, to select the proper winding arrangement and to sort out the optimum winding layout.

The application **FastMMF** becomes very useful tool at present owing to special types of electrical machines (like PM machines) that is more and more used in many applications and that uses tooth-concentrated windings, fractional-slot windings, multi-layer windings and other new type windings. This application has a user-friendly interface with minimum input data and it can be used on PC Tablet too.

REFERENCES

1. F. Magnussen, H. Lendenmann, *Parasitic Effects in PM Machines with Concentrated Winding*, IEEE Ind. Appl., **43**, 5, pp. 1223–1232, 2007.
2. F. Magnussen, C. Sadarangani, *Winding factors and Joule losses of permanent magnet machines with concentrated windings*, Proc. IEEE International Electric Machines and Drives Conference (IEMDC'03), vol. 1, pp. 333 – 339, 2003.
3. F. Libert, J. Soulard, *Investigation on Pole-Slot Combinations for Permanent-Magnet Machines with Concentrated Windings*, Proc. International Conference on Electric Machines (ICEM), paper ID 530, 5-8 Sept. 2004, Cracow, Poland.
4. P. Salminen, J. Mantere, J. Pyrhönen, M. Niemelä, *Performance analysis of fractional slot wound PM-motors*, Proc. International Conference on Electric Machines (ICEM), Paper ID 509, 5–8 Sept. 2004, Cracow, Poland.
5. A. M. El-Refäie, *Fractional-Slot Concentrated-Windings Synchronous Permanent Magnet Machines: Opportunities and Challenges*, IEEE Transactiona in Industrial Electronics, **57**, 1, pp. 107–121, 2010.
6. N. Bianchi, S. Bolognani, E. Fornasiero, *An Overview of Rotor Losses Determination in Three-Phase Fractional-Slot PM Machines*, IEEE Trans. on Ind. Appl., **46**, 6, pp. 2338–2345, 2010.
7. E. Fornasiero, L. Alberti, N. Bianchi, S. Bolognani, *Considerations on Selecting Fractional-Slot Nonoverlapped Coil Windings*, IEEE Ind. Appl., **49**, 3, pp. 1316–1324, 2013.
8. H. N. Phyu, N. L. H. Aung, C. Bi, *Influence of Winding Structure and the Effect of MMF Harmonics to the Spindle Motor Performance for Ultrahigh TPI HDD*, IEEE Trans. on Magnetics, **49**, 6, pp. 2776–2781, 2013.
9. L. Alberti, N. Bianchi, *Theory and Design of Fractional-Slot Multilayer Windings*, IEEE Trans. on Ind. Appl., **49**, 2, pp. 841–849, 2013.
10. I. R. Smith, J. M. Layton, *Harmonic elimination in polyphase machines by graded windings*, Proc. I.E.E., **110**, 9, pp. 1640–1648, 1963.
11. H. Grop, J. Soulard, H. Persson, *Theoretical investigation of fractional conductor windings for AC-machines - Definition, air-gap m.m.f. and winding factors*, Proc. of 18th International Conference on Electrical Machines (ICEM), Paper ID 1117, 2008.
12. D. A. Kocabas, *Novel Winding and Core Design for Maximum Reduction of Harmonic Magnetomotive Force in AC Motors*, IEEE Transactions on Magnetics, **45**, 2, pp. 735–746, 2009.
13. Fei Xiong, Xuefan Wang, *Design of a Low-Harmonic-Content Wound Rotor for the Brushless Doubly Fed Generator*, IEEE Transactions on Energy Conversion, **29**, 1, pp. 158–168, 2014.
14. M.V. Cistelecan, Mircea Popescu, Mihail Popescu, *Study of the Number of Slots/Pole Combinations for Low Speed Permanent Magnet Synchronous Generators*, Proc. of IEEE International Electric Machines & Drives Conference (IEMDC '07), Vol. 2, pp. 1616–1620, Antalya, 2007.
15. M. V. Cistelecan, H. Baris Cosan, M. Popescu, *Tooth Concentrated Fractional Windings for Low Speed Three Phase a.c. Machine*, Proc. of 17th International Conference on Electrical Machines, (ICEM) Paper ID 362, 2006.
16. I. Boldea, S.A. Nasar, *The Induction Machine Handbook*, CRC Press, Boca Raton, 2002.
17. B. Heller, V. Hamata, *Harmonic Field Effects in Induction Machines*, Elsevier Scientific, Amsterdam, 1977.
18. N. Bianchi, S. Bolognani, M. Dai Prè, G. Grezzani, *Design considerations for fractional-slot winding configurations of synchronous machines*, IEEE Transactions on Industry Applications, **42**, 4, pp. 997–1006, 2006.

Received June 8, 2016